Single Event Effect Rate Analysis and Upset Characterization of FPGA Digital Signal Processors

Roberto Monreal
Space Sciences, Southwest Research Institute
San Antonio, Texas, U.S.A.
rmonreal@swri.edu

Gary Swift, Y.C. Wang
Xilinx, Inc.
San Jose, California, U.S.A.

Michael Wirthlin, Brent Nelson
NSF Center for High Performance Reconfigurable Computing (CHREC),
Brigham Young University,
Provo, Utah, U.S.A.

***Abstract*—Charged particle induced upsets in the operation of Digital Signal Processors (DSP) are analyzed for on-orbit upset rate estimates. DSPs embedded in configuration hardened and non-hardened Field Programmable Gate Arrays (FPGA) are both studied for proton and heavy ion effects. The results reinforce the importance on the resulting upset rate of the mathematical fit parameters extracted from the experimental data.**

Keywords—Digital Signal Processors (DSP); Field Programmable Gate Array (FPGA); Single Event Effects (SEE)

I. INTRODUCTION

Digital Signal Processors (DSPs) are devices that provide real-time arithmetic computational capability to digital systems. They are available in standalone devices or can be found embedded in micro-processors and Field Programmable Gate Arrays (FPGA), and can be built into Application Specific Integrated Circuits (ASICs). The DSPs available in re-configurable FPGAs are especially useful to applications that are only realized by the capability of reprogrammable algorithms, such as implementation of ever-changing imaging and communication standards, and of course by the massive parallel capability offered by the nature of the FPGA architecture, where this inherent parallelism allows for considerable computational bandwidth while operating at moderate frequencies.

The real-time processing capability of FPGA-based DSP systems is also attractive to space-based system developers for commercial, scientific and military applications. The susceptibility of DSP FPGA applications to Single Event Effects (SEE) while on-orbit, expressed in upsets events per a unit of time, is of paramount importance and must be well understood to determine if, first, their level of susceptibility is acceptable, and secondly, if specific FPGA design techniques must be followed for their safe deployment in the space environment. For this reason, SEE test results from fuse-based FPGA DSPs [1] and RAM-based FPGA DSPs [2], [3] have been presented at various radiation effects and FPGA related conferences. Heavy-ion results [2] [3] of Xilinx Virtex FPGA DSPs demonstrate what appears to be a tolerable upset rate in GEO (Geosynchronous Earth Orbit), but what tolerance level is appropriate, is ultimately determined by the specific application. Furthermore, many common DSP applications, such as finite impulse response (FIR) filters, which cascade numerous DSP elements together, can employ a significant number of DSP elements. This often results in an increase in the application's SEE susceptibly, since the upset rate of an individual DSP element is then multiplied, magnifying the impact of the individual DSP susceptibility. Thus extracting accurate on-orbit upset rate estimates becomes a critical step in the DSP FPGA application susceptibility analysis.

In this write-up, the SEE data for Xilinx space-grade FPGA DSPs is reviewed, which includes the latest analysis on the Virtex-4QV heavy ion data and Virtex-5QV proton test results; which have also been released in [4]. This is followed with the results of an upset rate analysis study performed with two different automatic fitting methods to the newly acquired Virtex-5QV DSP proton, and the re-analyzed Virtex-4QV DSP heavy-ion data, originally presented in [2]. This study was undertaken in the effort to determine what the impact of the curve fitting method is on the resulting rate estimate of two different fitting approaches.

II. BACKGROUND

A. Virtex FPGA DSPs

The space-grade Xilinx Virtex-4QV and Virtex-5QV RAM-based FPGAs provide hundreds of DSP cells to the FPGA designer, each with the capability for several 48-bit wide input operators and a 48-bit output operand. The Xilinx Virtex-4QV is based on 90-nm CMOS technology, while the Virtex-5QV FPGA is 65-nm, and both are based on a non-RHBD (Rad-Hard by Design) process. They are arranged in columns across the device, as shown in Fig. 1, which

Manuscript received August 4, 2013. This work was supported in part by Xilinx Inc., under a contract between Xilinx Inc. and the Southwest Research Institute, and by the Southwest Research Institute Space Sciences Dept.

978-1-4799-1139-4/13/$31.00 ©2013 IEEE

illustrates the Virtex-5QV architecture interface of DSP cells with the Global Routing Matrix (GRM) cells. This provides the FPGA application designer with the capability of having real-time access to sophisticated mathematical computations. Each DSP cell is essentially a configurable logic block specially wired for real-time mathematical operations in between two bit-vector operators; where the operation type and operator are selected by the user through the FPGA fabric. The Virtex FPGA DSPs are outfitted with pipe-line registers, allowing these operations to take place at relatively high frequencies.

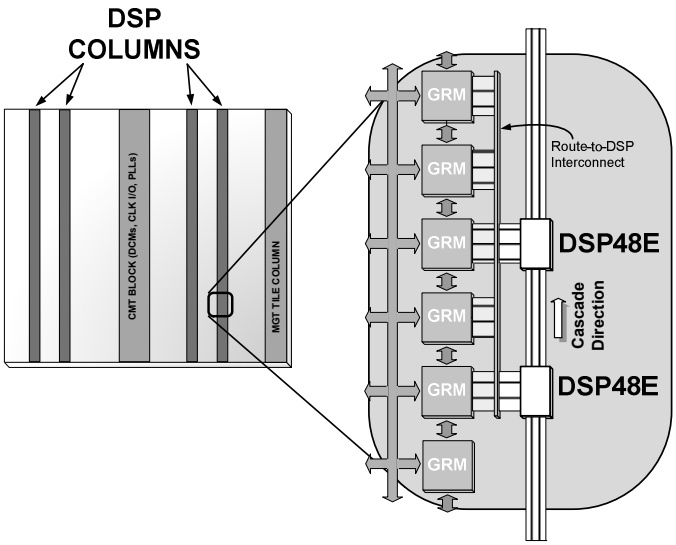

Fig. 1. DSP cell arrangement in a Virtex-5QV FX-130T device; with two of the 320 available DSP cells shown in detail.

B. DSP SEE Experimental Data

Virtex-4QV DSP heavy ion data was obtained at the Texas A&M Cyclotron in 2008 and 2009, and the Virtex-5QV DSP proton data was obtained at the University of California-Davis Crocker Nuclear Laboratory in 2012. Both the Virtex-4QV and Virtex-5QV DSP tests employed the setup used by the Xilinx Radiation Test Consortium (XRTC), which is illustrated in Fig. 2. The setup consists of an FPGA under-test (DUT), supported by a configuration manager FPGA performing the configuration maintenance and scrubbing during irradiation, and a second FPGA performing functional test verification duties. Two tests were generated, a static and a dynamic test. The static test provided all of the DSP register static test data, which showed how the DSP multiplier register possesses an enhanced susceptibility with regard to the other DSP registers [3].

For the dynamic tests, the infinite number of applications that DSP is capable of was reduced to three different applications that employed the basic functions of the DSP, which are multiplication, addition/subtraction, and accumulation functions. The dynamic tests exercised three DSPs simultaneously, monitoring the outputs of the DSP and measuring the duration and the time at which each upset occurred during irradiation. By monitoring the duration, upsets due to corruption from the configuration image vs. upsets due to the susceptibility of the functional plane could be separated. And by monitoring the duration time of each upset, upsets that are sourced in the global aspects of the DUT design, such as clock tree and input/output structures could also be extracted from the dynamic tests [3].

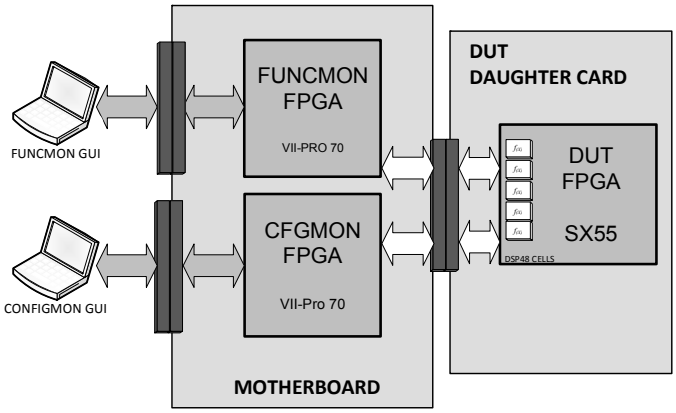

Fig. 2. XRTC DSP SEE Test Experimental Setup

C. Upset Rate Calculations

To understand the susceptibility of an electronic device to the charged-particle or radiation environment of space, engineers and scientists make use of experimentally obtained SEE cross-section for a given device vs. incident particle energy. This data is then used to estimate the on-orbit upset rate of the device. This estimation helps in determining, first of all, if the device will survive and function correctly in the space environment, and secondly, if any mitigation or particular implementation methods must be employed to ensure its safe deployment in the mission. Much work by industry and academia has been done that both demonstrates and evaluates the accepted methods of doing so. Summarizing these methods, the on-orbit upset rate is essentially calculated by integrating the flux of particles found in the intended space environment over the susceptibility of the device to radiation. The device susceptibility is defined by a theoretical volume within the electronic device material that characterizes the critical charge needed to cause an upset. The susceptibility of this sensitive volume to incident particle energy is further defined by an upset cross-section per unit area vs. energy. The demonstration and details of this calculation are beyond the scope of this write up, but many references exists that can be consulted [5].

To obtain the on-orbit upset rates, the community has developed software applications that help define the space charged-particle environment and also perform the integration. Two applications are CRÈME-MC [1] (U.S.), and OMERE [2] (Europe), which are widely used and easily accessible. Common to both of these applications is the ability for the user to specify and generate environmental models tailored for the particular mission of interest and to input either the actual cross-section experimental test data or mathematical approximation parameters that define the device susceptibility. Another upset rate estimation tool exists, developed by the Jet Propulsion Laboratory (JPL) and made available to the authors

[1] https://creme.isde.vanderbilt.edu/
[2] http://www.trad.fr/OMERE-Software.html

through participation in the XRTC, which can also generate heavy ion upset rate estimates. The JPL upset rate estimation tool is unique in that it can provide to the user a feedback on the contribution of each Linear Energy Transfer (LET) to the overall upset rate estimate calculated for the device in terms of percent contribution vs. LET.

D. Weibull Curve Fit to SEE data

To perform the integration calculation, analysts make use of a Weibull mathematical function, which is a continuous probability distribution function. This allows for the upset rate integration to be done across all the possible incident particle energies of the intended space environment. The demonstration and details of the Weibull approximation method are also beyond the scope of this write-up and many sources also exist that can be referenced [6] [7]. Summarizing, the Weibull approximation of the SEE experimental data for a device is defined by 4 parameters: (1) the particle energy threshold or resulting LET threshold, the energy amount upon which the device becomes susceptible to SEEs (LET_{th}, or $E_{P\text{-th}}$); (2) the cross-section at which the device's susceptibility saturates (σ_{SAT}), defined per unit area (cm^{-2}); and the rate of increase in susceptibility with increasing energy, defined by (3) the unit-less exponent parameter (S), and (4) the width parameter (W), with units of $MeV \cdot cm^2/mg$ for heavy ions and MeV for protons. The formula for the Weibull function used to approximate a cross-section vs. energy data set is shown below:

$$F(x) = \sigma_{SAT} (1 - \exp \{ - [(x - x_o) / W]^S \}) \qquad (1)$$

Where x is the given particle energy, x_o is the threshold particle energy (LET_{th}, or $E_{P\text{-th}}$), both with units of $MeV \cdot cm^2/mg$ for heavy ions and MeV for protons. The resulting distribution approximation is intended to provide the susceptibility cross-section across all energies for the device tested. As can be inferred, the parameter definition is a key step in obtaining an accurate upset rate estimate.

Fitting Weibull parameters to a raw set of experimental data is a nearly arbitrary exercise, with the radiation effects analyst usually generating the fit by hand, or generating their own software (SW) application to assist in generating the fit parameters. Thus having a convenient and consistent method would reduce the risk of miscalculating the on-orbit upset rates due to inconsistent fits. The OMERE upset rate application is very useful since it provides the user access to an automatic fitting application, however not much is known about the internal algorithm that generates the fit parameters. A SW application also available through the author's participation in the XRTC, is SERET (Single Event Rate Estimation Tool), developed by Brigham Young University in the Center for High-Performance Reconfigurable Computing (CHREC). Its purpose is to fit experimental data to a Weibull curve in an automated fashion. The curve fit is done using modified least squares algorithms where the "fit" calculated is done with a weighting factor applied. The weighting factor is computed from three things: (1) more weight is given to lower LET points in the region before saturation of the curve, (2) more weight is given to points that fall below the computed curve, and (3) more weight is given to data points with smaller error bars. In addition to providing an automated fit, this application also provides the user the capability to interactively modify the resulting curve fit as desired to obtain the most accurate fit possible.

Table I. OMERE and SERET Weibull fit parameters.

Device, particle	DSP Test	Upset Type	No. Data Pts.	OMERE Fits				SERET Fits			
				$E_{p\text{-}th}$ or LET_{th}	σ_{SAT}	*W*	*S*	$E_{p\text{-}th}$ or LET_{th}	σ_{SAT}	*W*	*S*
Virtex-4QV; Heavy Ions	A/B Register Static	Bit	9	0.001	3.67×10^{-8}	25.7	1.503	0.100	1.16×10^{-7}	151.4	0.978
	C Register Static	Bit	9	0.001	2.90×10^{-8}	13.7	1.836	0.100	8.59×10^{-7}	414.5	1.197
	M Register Static	Bit	9	0.001	8.60×10^{-8}	16.2	1.518	0.100	4.41×10^{-7}	256.6	0.868
	P Register Static	Bit	9	0.001	7.28×10^{-8}	23.0	1.982	0.100	8.59×10^{-7}	411.4	1.197
	Addition Dynamic	Config.	4	0.001	2.76×10^{-5}	9.9	1.832	0.100	1.78×10^{-4}	133.0	1.087
	Multiplication Dynamic	Config.	4	0.001	1.42×10^{-5}	8.3	1.652	0.100	1.24×10^{-5}	8.4	1.307
	Addition Dynamic	Func.	4	0.001	3.46×10^{-6}	9.1	1.827	0.100	1.78×10^{-4}	375.0	1.197
	Multiplication Dynamic	Func.	4	0.001	4.20×10^{-6}	10.7	1.983	0.100	1.78×10^{-4}	500.0	1.197
	A/B Register Static	Reg.	9	0.001	6.54×10^{-7}	25.8	1.505	0.100	3.26×10^{-6}	269.8	0.978
	C Register Static	Reg.	9	0.001	1.39×10^{-6}	14.6	1.819	0.100	4.69×10^{-5}	500.0	1.197
	M Register Static	Reg.	9	0.001	1.61×10^{-6}	16.5	1.497	0.100	6.35×10^{-6}	243.5	0.813
	P Register Static	Reg.	9	0.001	1.78×10^{-6}	20.5	1.742	0.100	1.24×10^{-5}	447.4	0.978
Virtex-5QV; Protons	C Register Static	Bit	3	17.999	3.76×10^{-14}	0.05	0.235	4.000	3.52×10^{-14}	16.7	1.865
	M Register Static	Bit	3	17.999	1.36×10^{-12}	0.01	0.198	4.000	1.31×10^{-12}	15.1	2.189
	P Register Static	Bit	3	17.999	3.00×10^{-14}	0.01	0.190	4.000	2.87×10^{-14}	15.1	2.625
	Addition Dynamic	Func.	2	18.799	7.41×10^{-12}	0.01	0.194	4.000	8.00×10^{-12}	19.4	0.901
	Multiplication Dynamic	Func.	2	18.799	8.94×10^{-12}	0.01	0.127	4.000	1.10×10^{-11}	10.1	0.298
	C Register Static	Reg.	3	17.999	1.73×10^{-12}	0.10	0.260	4.000	2.20×10^{-12}	27.8	1.325
	M Register Static	Reg.	3	17.999	2.51×10^{-12}	0.01	0.199	4.000	2.99×10^{-12}	19.01	1.353
	P Register Static	Reg.	3	17.999	1.34×10^{-12}	0.01	0.190	4.000	1.77×10^{-12}	23.20	1.146

III. Weibull-Fit Upset-Rate Study

A. DSP Weibull Fits

As stated, two types of automated Weibull-fitting algorithms were used in the study, SERET and the Weibull fitting application provided by OMERE. The fits were generated for the dynamic and static test cross-sections vs. LET and energy obtained for the Virtex-4QV DSPs with heavy ions, and the Virtex-5QV DSPs with protons. The experimental tables with the measured cross-section vs. LET were fed into each of the fit application to obtain the fit parameters, and these are shown in Table I. In general, there are several consistent differences in between the SERET and OMERE fits that can be noticed, particularly for the heavy ion fits. The most prominent is the LET_{th}, which is picked arbitrarily by each algorithm, where OMERE fits to 0.001 and SERET to 0.1MeV·cm^2/mg. The σ_{SAT} is also considerably different, and SERET always fits consistently higher than OMERE, ranging in between a factor of 3 and 50 in difference. The W parameter is also substantially different, which OMERE always fits below a value of 25, but SERET can fit as high as 500MeV·cm^2/mg. And finally, the exponent parameter S, which defines the initial cross-section response of the test data with increasing LET, is also shown to be consistently smaller for the SERET fits. The resulting discrepancy in between the OMERE and SERET fits is illustrated in Fig. 3 and Fig. 4 for two of the Virtex-4QV DSP SEE manifestations.

For the proton fits, the lack of a well defined, measured threshold proton energy requires an arbitrary selection of the threshold energy. In this study, OMERE picked a threshold energy right below the lowest E_P at which a cross-section point was measured. For the SERET fits, an arbitrary threshold energy of 4.0MeV was chosen, since this is the threshold proton energy used in [4]. As opposed to the heavy ion fits, both SERET and OMERE are in relatively good agreement on the saturated cross-section parameter, but differ significantly in the W and S definitions. This is because OMERE is using a much higher E_P threshold, which results in a Weibull curve with the shape of a step function; while the SERET Weibull curve can be more gradual towards the lower E_P threshold, as is shown in Fig. 5.

B. Rate Analysis

To compare the results of each fit approach for the different DSP SEE manifestations, on-orbit upset rates were extracted for each Weibull using CRÈME-MC. For the heavy ion data, the environment used is a Geosynchronous orbit (GEO), while for the proton data, a circular 800km orbit is used. The environmental settings used in the rate calculations with CRÈME-MC are shown in Table II. The on-orbit upset rate results generated are shown in Table IV for the heavy ions and Table V for protons.

As expected from the higher saturated cross-section parameter generated by the SERET heavy ion fits, the resulting rate is also consistently higher than the OMERE fits. But examining closer, the difference in the saturated cross-section does not correspond to the difference in the resulting rate. The ratios of the saturated cross-section parameters and the upset rates are shown in the right-most columns of Table IV. This is particularly true for the Virtex-4QV dynamic functional upset data, where saturated cross-section differences by factors of 40 and 50 result in on-orbit rate differences by less than a factor of 2. This is also evident in some of the static upset rates, where a saturated cross-section difference with a factor of 12 results in an on-orbit rate difference with a factor of 3.

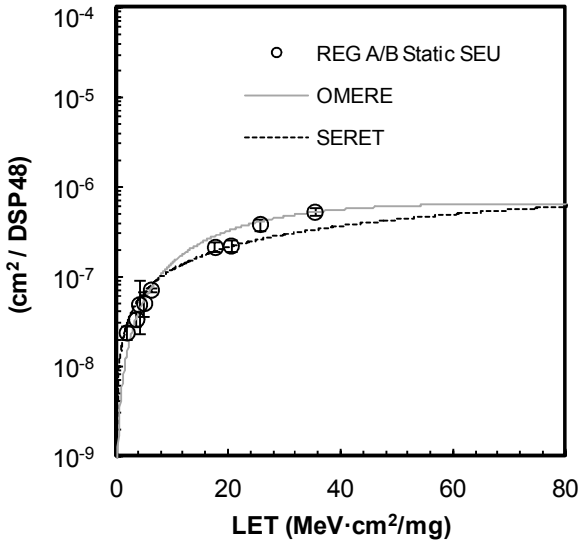

Fig. 3. OMERE and SERET Weibull fits for Static Heavy Ion Data of Virtex-4QV DSP A/B Input Register Upsets.

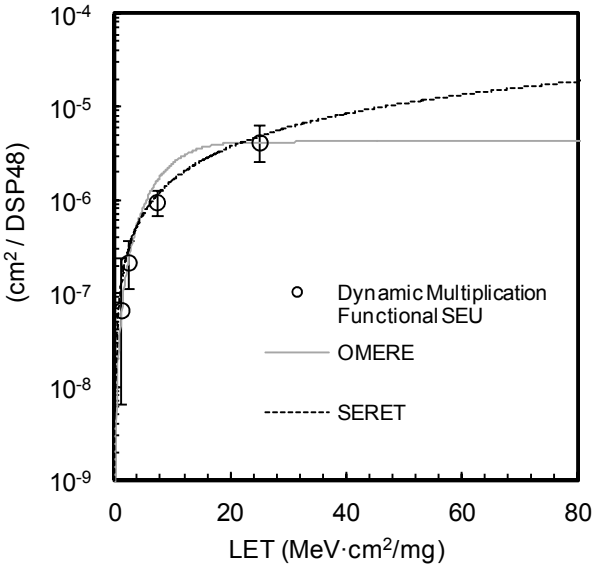

Fig. 4. OMERE and SERET Weibull fits for Heavy Ion Dynamic Data of the Virtex-4QV DSP Multiplication operation functional upsets.

Thus, in general, since the sensitive volume dimensions used in the rate calculation are defined by the heavy ion

saturated cross-section, the on-orbit upset rate tends to follow the saturated cross-section parameter, but as seen with some of the DSP dynamic and static data, some notable exceptions exist where it can be seen that the other Weibull parameters are equally or more important to the upset rate.

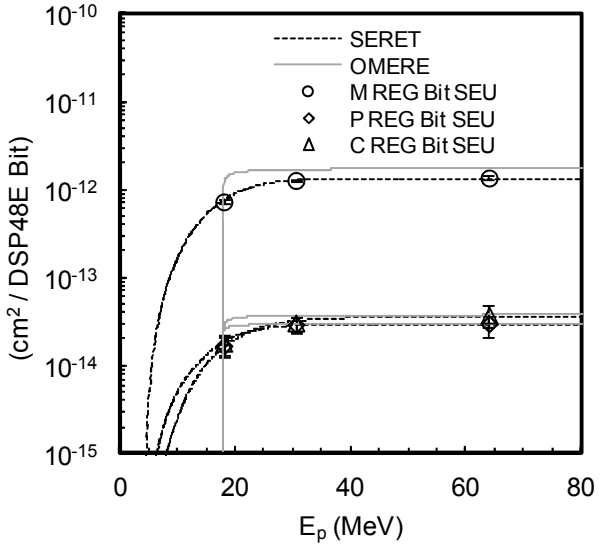

Fig. 5. OMERE and SERET Weibull fits for Static Proton Data of the Virtex-5QV DSP M, P and C Registers.

This general statement regarding the saturated cross-section appears to be even truer for proton upset rate calculations, where the cross-section defines the on-orbit upset rate with a small impact on the upset rate from the other fit parameters. It must be noted that the CRÈME-MC on-orbit proton rates generated only take into account the spoliation effects and not direct-ionization effects caused by protons, thus the protagonism of the saturated cross-section parameter in the proton rate calculations.

C. Weibull Fit Quality

In order to determine the quality of each Weibull fit to the experimental data, a variation of the Kullbak-Leibler divergence theorem can be applied [5]. The Kullbak-Leibler divergence (D_{KL}) theorem is a non-symmetric measure of the difference between two distributions, where one is "real" and the other theoretical. This divergence is typically used in communications theory, and in this case, it is applied to understand the difference between the experimental data distribution and the two Weibull distributions applied. The Kullbak-Leibler divergence theorem is defined as follows:

$$D_{KL}(P||Q) = \Sigma_i \, (\ln (P(i)/Q(i)) \, P(i)) \qquad (2)$$

Where P is the experimental or "real" distribution and Q is the Weibull or theoretical distribution. The values of the divergence are unit-less, and increase in magnitude with a corresponding larger divergence. The quality of fit for each data point (i), a subset of the data points, or the entire data set can be rated with the D_{KL} theorem. Since the sum of two equal but opposite divergences can equate to zero, Equation (2) can be modified to eliminate the negativity of natural log coefficient by summing the absolute values of the divergence calculation of each data point.

The divergence calculations are shown in Table VI for the Virtex-4QV DSP heavy ion data. The Weibull fits for the Virtex-5QV DSP proton data were shown to have a more consistent agreement regardless of fit parameters, and thus were spared from divergence calculations. Divergence scores were generated for the entire set of data points of each test, and for the data points obtained at LET values less than 10MeV·cm^2/mg of each test. The SERET fit at LET values less than 10MeV·cm^2/mg results in less of a divergence than the OMERE tests for all of the test data, except for the A/B register tests, which OMERE fits more accurately but by a very small margin (1.59 and 1.33, for per bit and per register data respectively). The divergence margin of the SERET fits over the OMERE fits on the other hand can be as much as an order of magnitude in some cases, such as for the Dynamic Multiplication tests and the P Register Static tests.

Table II. CRÈME-MC input parameters used in on-orbit rate calculations.

Parameter	Setting
Orbit (Heavy Ions)	Geosynchronous
Orbit (Protons)	800km circular, 90° inclination
Particle atomic no. range	1 to 92
Trapped Proton Model	AP8MIN
GCR Model	CRÈME96
Solar Conditions	Quiet
Geomagnetic Transmission Function	Yes (for Protons)
Geomagnetic Weather	Quiet
Shielding	0.1" Aluminum
LET Spectrum atomic no. range	1 to 92
Minimum particle energy	0.1MeV/nuc

When observing the divergence of the fits across all of the data points, both of the OMERE and SERET fits appear to offer approximately the same quality of fit. This leads to the conclusion that the OMERE fit treats each LET data point with approximately the same rigor in the fitting algorithm. And, as can be seen in Fig. 3 and Fig. 4, it also determines the saturated cross-section parameter by directly taking the cross-section data point at the highest LET. The SERET fitting algorithm, by considering the data points at LETs below the "knee" section of the Weibull curve to be more important in the fitting exercise, emphasizes the fit to experimental data points that have a much higher impact on the resulting upset rate, thus resulting in a higher quality fit at LETs below 10MeV·cm^2/mg.

Divergence scores were generated for the LET points less than 10MeV·cm^2/mg because the device susceptibility at the lower LETs is more persuasive in the upset rate estimate than the susceptibility from LETs higher than 10MeV·cm^2/mg. This LET value was inferred to with help of the JPL SEU rate estimation tool, since this is the LET point upon which the fractional contribution to the total upset becomes approximately less than 1.0% of the total upset rate. This point is illustrated in Fig. 7 and Fig. 6, which show the contribution

to the upset rate calculated from each LET value using both, the OMERE and SERET Weibull approximation fit parameters, and using the actual experimental data cross-section points, shown as a step function in Fig. 8 and Fig. 9; the actual cross-section data points for these data sets are shown in III. Only the A/B Static Register upsets and the Multiplication Dynamic functional upsets data sets are used as an example to focus on. The upset contributions from each of the experimental data point's cross-section vs. LET results in a step function at each LET point. The rate contribution from the LETs less than 10MeV·cm^2/mg is clearly shown in Fig. 8 and Fig. 9 to have the most significant contribution to the overall upset rate, while the fractional contribution to the upset rate decreases rapidly with increasing LET. This is true for the two Weibull fit methods. The step-function of the fractional upset-rate contribution generated from the discrete experimental points indicates that virtually the entire upset rate is attributed to the susceptibility of the lowest LET cross-section data point.

Table III. Experimental Cross-Sections for A/B Static Regiter Upset and Multiplication Dynamic Functional Upset Data

A/B Static Register Upset Data		Multiplication Dynamic Functional Upset Data	
LET (MeV·cm^2/mg)	**Cross-Section** (/cm^2)	**LET** (MeV·cm^2/mg)	**Cross-Section** (/cm^2)
35.3	5.34x10^{-7}	25.0	4.21x10^{-6}
25.6	3.90x10^{-7}	7.3	9.60x10^{-7}
20.4	2.24x10^{-7}	2.4	2.17x10^{-7}
17.6	2.16x10^{-7}	1.2	6.67x10^{-8}
6.2	7.22x10^{-8}		
5.0	5.13x10^{-8}		
4.1	4.95x10^{-8}		
3.6	3.39x10^{-8}		
1.9	2.41x10^{-8}		

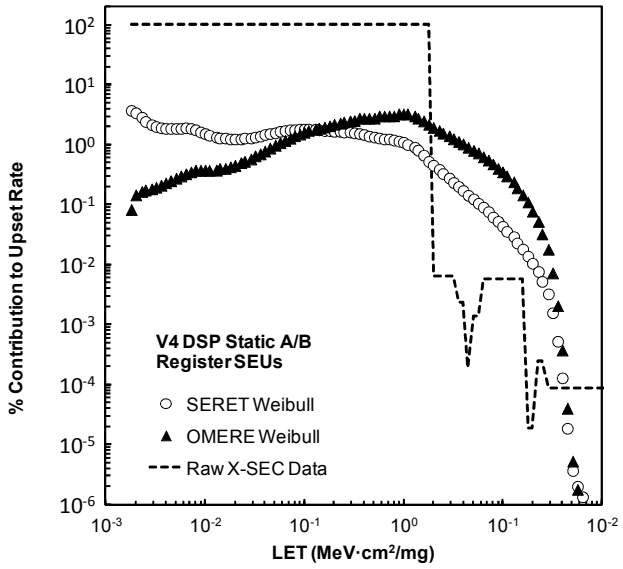

Fig. 6. Percentage contribution of each LET to the overall on-orbit rate for the Virtex-4QV DSP Static A/B Register SEU data.

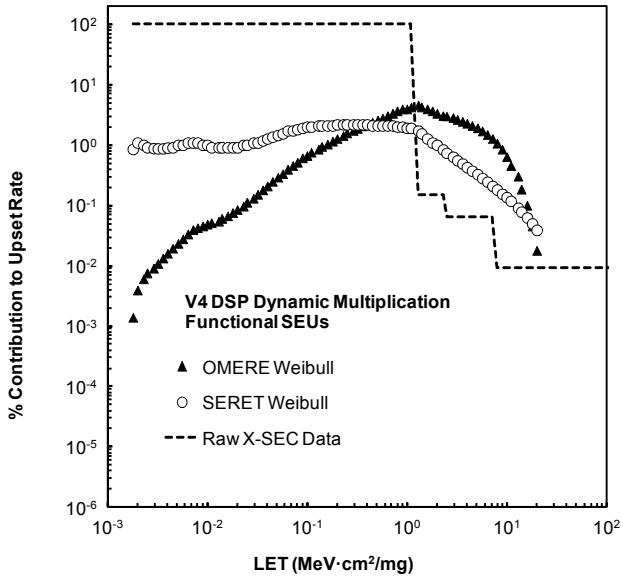

Fig. 7. Percentage contribution of each LET to the overall on-orbit rate for the Virtex-4QV DSP Dynamic Multiplication Functional SEU data.

IV. Conclusions

The results of this study demonstrate that the fitting approach employed to extract the Weibull parameters from heavy ion experimental data can vary the upset rate results in what at first appears to be a negligible upset rate difference. But with some real applications employing hundreds of FPGA elements like DSPs, the small rate difference from a single element or DSP perspective can quickly become a difference of several orders of magnitude. And if taking into account the effects of harsher radiation conditions, such as the presence of solar event particles, the on-orbit upset rate calculation variances are even more pronounced [9]. Furthermore, if using upset rate calculations from experimental data to compare the impact in between different FPGA upset mechanisms, or different design approaches or mitigation techniques, non-consistent fits can lead to inaccurate upset rates and therefore provide ill comparisons. For proton spoliation rate estimates, the impact of different Weibull fitting methods appears to be much less significant than for heavy ions.

The study also demonstrates that Weibull fits which determine the saturated cross-section parameter by first focusing on the cross-section value of the highest LET data point, may result in compromising the fit at the more critical LET values to the upset rate calculation, which for the Virtex-4QV DSPs can be considered to be below 10MeV·cm^2/mg. Such a fitting approach will more than likely result in a lower estimate calculation of the upset rate, but not due to the lower cross-section, but from an underestimate of the fit at the lower LET values. Automated Weibull fitting tools like SERET, which employ more sophisticated fitting algorithms that take into account data point LET values and error bars, and de-emphasize the fit to data points at the higher LETs, generate a Weibull curve that can better fit the lower LET data points, resulting in what is believed to be a more accurate on-orbit upset rate estimate. Ultimately, automated Weibull fits should weigh each of the data points to be fitted against by the actual

impact of the LET in the environment intended. This can be done by an iterative process, where the fractional contribution to the upset rate of each data point is first calculated, providing a "score" for each data point that reflects that actual impact of that energy or LET in the environment. These data point "scores" can be used as the weighing factor to drive the fitting algorithm. Such a Weibull fitting philosophy can be applied to the heavy ion test data of any device.

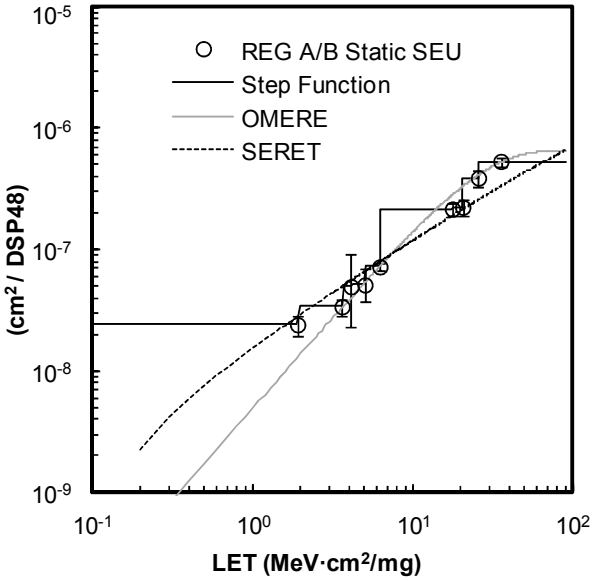

Fig. 8. Cross-Section Step Function, and OMERE and SERET Weibull fits, for the Virtex-4QV DSP A/B Input Register Heavy Ion Upsets.

Finally, this study can also serve to demonstrate the value of disclosing the contribution to the upset rate of the different LET energies used in the testing. This allows radiation analysts to understand what experimental points will impact the rate calculation the most, and thus can focus the fit of the Weibull to those data points. This information can also provide SEE experimentalists with the LET range that will most impact the upset rate in the specific environment that the device being tested is intended for, and thus can focus on those LET ranges during accelerator testing. Most upset rate calculation tools like OMERE and CRÈME-MC generate this information as an intermediate, internal step in their calculation process, but unfortunately do not disclose it to the user.

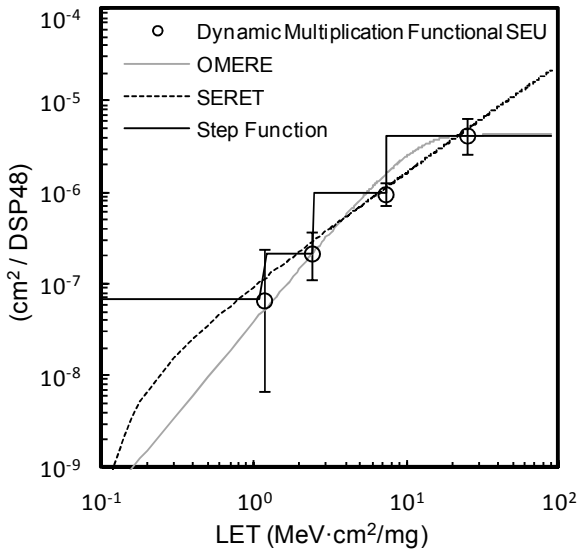

Fig. 9. Cross-Section Step Function, and OMERE and SERET Weibull fits, for the Virtex-4QV DSP Multiplication Operation Functional Upsets.

V. ACKNOWLEDGMENTS

The authors wish to acknowledge the members of the XRTC and CHREC for their help and insight in the execution of this study. The authors would also like to extend a special mention to Ray Ladbury of NASA-GSFC for providing guidance in the fit quality estimates, and to Greg Allen of JPL for allowing the use of the JPL SEU Rate estimation application.

Table IV. Virtex-4QV DSP Heavy Ion Upset Rates from OMERE and SERET Weibull fit parameters.

DSP Test	Upset Type	OMERE Fits		*SERET Fits*		*SERET vs. OMERE*	
		σ_{SAT}	*Upset Rate (/day)*	σ_{SAT}	*Upset Rate (/day)*	σ_{SAT} *Ratio*	Upset Rate Ratio
A/B Register Static	Bit	3.67×10^{-8}	2.10×10^{-7}	1.16×10^{-7}	5.09×10^{-7}	3.2	2.4
C Register Static	Bit	2.90×10^{-8}	1.68×10^{-7}	8.59×10^{-7}	4.56×10^{-7}	29.6	2.7
M Register Static	Bit	8.60×10^{-8}	1.05×10^{-6}	4.41×10^{-7}	2.36×10^{-6}	5.1	2.2
P Register Static	Bit	7.28×10^{-8}	1.56×10^{-7}	8.59×10^{-7}	4.60×10^{-7}	11.8	2.9
Addition Dynamic	Config.	2.76×10^{-5}	5.66×10^{-4}	1.78×10^{-4}	6.69×10^{-4}	6.4	1.2
Multiplication Dynamic	Config.	1.42×10^{-5}	4.75×10^{-4}	1.24×10^{-5}	5.23×10^{-4}	1.1	1.1
Addition Dynamic	Func.	3.46×10^{-6}	7.63×10^{-5}	1.78×10^{-4}	1.26×10^{-4}	51.4	1.6
Multiplication Dynamic	Func.	4.20×10^{-6}	6.09×10^{-5}	1.78×10^{-4}	8.94×10^{-5}	42.3	1.5
A/B Register Static	Reg.	6.54×10^{-7}	5.29×10^{-6}	3.26×10^{-6}	9.58×10^{-6}	5.0	1.8
C Register Static	Reg.	1.39×10^{-6}	1.43×10^{-5}	4.69×10^{-5}	2.31×10^{-5}	33.7	1.6
M Register Static	Reg.	1.61×10^{-6}	6.10×10^{-5}	6.35×10^{-6}	5.12×10^{-5}	3.9	1.2
P Register Static	Reg.	1.78×10^{-6}	1.25×10^{-5}	1.24×10^{-5}	2.28×10^{-5}	7.0	1.8

Table V. Virtex-5QV DSP Proton Upset Rates from OMERE and SERET Weibull fit parameters.

DSP Test	Upset Type	OMERE Fits		SERET Fits		*SERET vs. OMERE*	
		σ_{SAT}	Upset Rate (/day)	σ_{SAT}	Upset Rate (/day)	*σ_{SAT} Ratio*	Upset Rate Ratio
C Register Static	Bit	$3.76x10^{-14}$	$3.95x10^{-5}$	$3.52x10^{-14}$	$4.56x10^{-5}$	1.1	1.14
M Register Static	Bit	$1.36x10^{-12}$	$5.91x10^{-5}$	$1.31x10^{-12}$	$8.32x10^{-5}$	0.9	1.21
P Register Static	Bit	$3.00x10^{-14}$	$3.14x10^{-5}$	$2.87x10^{-14}$	$4.53x10^{-5}$	1.3	1.17
Addition Dynamic	Func.	$7.41x10^{-12}$	$1.63x10^{-4}$	$8.00x10^{-12}$	$2.49x10^{-4}$	1.0	1.53
Multiplication Dynamic	Func.	$8.94x10^{-12}$	$1.83x10^{-4}$	$1.10x10^{-11}$	$4.91x10^{-4}$	1.2	2.68
C Register Static	Reg.	$1.73x10^{-12}$	$8.68x10^{-7}$	$2.20x10^{-12}$	$9.92x10^{-7}$	1.2	1.15
M Register Static	Reg.	$2.51x10^{-12}$	$3.20x10^{-5}$	$2.99x10^{-12}$	$3.89x10^{-5}$	1.0	1.41
P Register Static	Reg.	$1.34x10^{-12}$	$7.03x10^{-7}$	$1.77x10^{-12}$	$8.22x10^{-7}$	1.3	1.44

Table VI. Kullbak-Leibler Divergence calculations for OMERE and SERET Weibull fits to Virtex-4QV DSP data.

DSP Test	Upset Type	OMERE Fits		SERET Fits		Optimal Fit, margin *(all data)*	Optimal Fit, margin *(LET < 10)*
		D_{KL} *(all data)*	D_{KL} *(LET < 10)*	D_{KL} *(all data)*	D_{KL} *(LET < 10)*		
A/B Register Static	Bit	$1.16x10^{-8}$	$1.83x10^{-9}$	$1.54x10^{-8}$	$2.91x10^{-9}$	OMERE, 1.33	OMERE, 1.59
C Register Static	Bit	$2.09x10^{-8}$	$1.20x10^{-8}$	$2.84x10^{-8}$	$1.04x10^{-8}$	OMERE, 1.36	SERET, 1.15
M Register Static	Bit	$5.33x10^{-8}$	$1.27x10^{-8}$	$3.77x10^{-8}$	$7.84x10^{-9}$	SERET, 1.41	SERET, 1.62
P Register Static	Bit	$5.05x10^{-8}$	$5.85x10^{-9}$	$5.00x10^{-8}$	$3.98x10^{-9}$	SERET, 1.01	SERET, 1.47
Addition Dynamic	Config.	$5.83x10^{-6}$	$5.74x10^{-6}$	$3.88x10^{-6}$	$2.85x10^{-6}$	SERET, 1.50	SERET, 2.01
Multiplication Dynamic	Config.	$2.10x10^{-6}$	$2.08x10^{-6}$	$3.23x10^{-6}$	$1.08x10^{-6}$	OMERE, 1.54	SERET, 1.39
Addition Dynamic	Func.	$6.90x10^{-7}$	$6.87x10^{-7}$	$2.84x10^{-6}$	$5.04x10^{-7}$	OMERE, 4.11	SERET, 1.36
Multiplication Dynamic	Func.	$7.03x10^{-6}$	$2.55x10^{-6}$	$8.22x10^{-7}$	$2.25x10^{-7}$	SERET, 8.55	SERET, 11.33
A/B Register Static	Reg.	$2.05x10^{-7}$	$2.89x10^{-8}$	$2.81x10^{-7}$	$3.17x10^{-8}$	OMERE, 1.10	OMERE, 1.37
C Register Static	Reg.	$1.27x10^{-6}$	$6.19x10^{-7}$	$1.31x10^{-6}$	$5.28x10^{-7}$	OMERE, 1.03	SERET, 1.17
M Register Static	Reg.	$1.10x10^{-6}$	$2.61x10^{-7}$	$1.01x10^{-6}$	$1.61x10^{-7}$	SERET, 1.62	SERET, 1.09
P Register Static	Reg.	$9.78x10^{-6}$	$2.35x10^{-6}$	$1.56x10^{-6}$	$1.56x10^{-7}$	SERET, 6.26	SERET, 15.09

VI. REFERENCES

[1] C. Perez, M. Berg and M. R. Friendlich, "Single-Event Effects Testing of Embedded DSP Cores within Microsemi RTAX4000D FPGA Devices," in *ReSpace/MAPLD Conference Proceedings*, Albuquerque, NM, 2011.

[2] R. M. Monreal, C. Carmichael, C.-W. Tseng, G. Swift, G. Miller and G. Allen, "Interaction of Ionized-Particles with Advanced Signal Processing Devices in Field-Programmable Gate Arrays and Development of Mitigation Techniques," in *Proceedings of the 2009 MAPLD Conference*, Greenbelt, MD, 2009.

[3] R. M. Monreal and G. Swift, "Upset Manifestations in Embedded Digital Signal Processors due to Single Event Effects," in *RADECS 2012, Conference Proceedings*, Biarritz, France, 2012.

[4] G. Swift and G. Allen, "Virtex-5QV Architectural Features SEU Characterization Summary," Xilinx Inc., San Jose CA, 2013.

[5] E. L. Petersen, J. C. Pickel, J. J. H. Adams and E. C. Smith, "Rate Prediction for Single Event Effects -- a Critique," *IEEE Transactions on Nuclear Science,* vol. 6, no. 39, pp. 1577-1599, December 1992.

[6] N. L. Johnson, S. Kotz and N. Balakrishnan, "Continuous Multivariate Distributions, Volume 1, Models and Applications, 2nd Edition," in *Probability and Mathematical Statistics: Applied Probability and Statistics (2nd ed.)*, New York, John Wiley & Sons, 1994.

[7] A. J. Tylka, W. F. Dietrich, P. R. Boberg, E. C. Smith and J. J. H. Adams, "Single Event Upsets Caused by Solar Energetic Heavy Ions," *IEEE Transactions on Nuclear Science,* vol. 43, no. 6, pp. 2758-2766, 1996.

[8] S. Kullback, *Information Theory and Statistics*, Dover Publications, 1997.

[9] R. Monreal, G. Swift, Y. Wang, M. Wirthlin, J. Walker and B. Nelson, "Upset Rate Estimate Analysis of Digital Signal Processors in FPGAs," in *Procedings of the 2013 SEE Symposium*, La Jolla, California, 2013.